

Synthesis, radiolabeling and in vivo biodistribution of diethylstilbestrol phosphate derivative (DES-P)

Perihan Ünak · F. Zümrüt Biber Müftüleri ·
Çiğdem İçhedef · E. İlker Medine · Kübra Özmen ·
Turan Ünak · Ayfer Yurt Kilçar · F. Gül Gümüşer ·
Yasemin Parlak · Elvan Sayıt Bilgin

Received: 20 November 2011 / Published online: 4 April 2012
© Akadémiai Kiadó, Budapest, Hungary 2012

Abstract Diethylstilbestrol (DES) is a well known, nonsteroidal estrogen with high affinity for the estrogen receptor (ER). Today DES is used to treat breast and prostate cancers. A phosphate derivative of DES [Diethylstilbestrol diphosphate (DES-P)] which is specific to tumor cells consisting alkaline phosphatase enzyme was synthesized and labeled with ^{99m}Tc using tin chloride as reducing agent. In vivo biological activity of ^{99m}Tc labeled diethylstilbestrol phosphate compound (^{99m}Tc -DES-P) was examined by biodistribution studies on Wistar Albino rats. Statistical evaluation was performed using SPSS 13 program. The percentage (%) radiolabeling yield of ^{99m}Tc -DES-P and quality control studies were done by Thin Layer Radio Chromatography (TLRC). Results showed that, ^{99m}Tc -DES-P may be proposed as an imaging agent for ER enriched tumors such as uterus and prostate and their metastases in bones.

Keywords Diethylstilbestrol (DES) · ^{99m}Tc labeled diethylstilbestrol diphosphate (^{99m}Tc -DES-P) · ^{99m}Tc -DES-P for receptor saturated studies (^{99m}Tc -Rec-DES-P) · Cancer imaging

P. Ünak · F. Z. Biber Müftüleri (✉) · Ç. İçhedef ·
E. İ. Medine · K. Özmen · A. Y. Kilçar
Department of Nuclear Applications, Institute of Nuclear
Science, Ege University, Bornova, Izmir, Turkey
e-mail: fazilet.zumrut.biber@ege.ed.tr

T. Ünak
Department of Chemistry, Faculty of Science,
Ege University, Bornova, Izmir, Turkey

F. G. Gümüşer · Y. Parlak · E. S. Bilgin
Department of Nuclear Medicine, School of Medicine,
Celal Bayar University, Manisa, Turkey

Introduction

It is known that the uterus, mammary gland, placenta, liver, central nervous system, cardiovascular system and bones have high ER α content and prostate, testis, ovary, thyroid gland, skin, lung and muscle contain ER β [1].

Prostate and breast cancers were reported that were most common cancer types [2]. Diethylstilbestrol (DES) is a synthetic nonsteroidal estrogen, being used to treat postmenopausal breast and advanced prostate cancer [3–5]. Diethylstilbestrol diphosphate (fosfestrol) is an inactive synthetic estrogen, used as a prodrug of the active DES that has phosphate substituted on both hydroxyl groups for localised, advanced and hormone refractory prostate cancer [6–10]. In other study the response of fosfestrol in bony metastases was very high [11, 12].

According to the College of American Pathologists, alkaline phosphatase enzyme is an important prognostic factor for patients with renal cell carcinoma. Although elevated enzyme activity usually prompts a search for bone and/or liver metastases, the analysis lacks specificity [13]. It is known that alkaline phosphatase enzyme is present in large amounts in bone in which it plays a role in mineralization [14–16]. This is why the synthesis compounds which undergo phosphorylation process (conjugation of phosphate group) come into question in the imaging and therapy of consisting alkaline phosphatase enzyme cancer types.

Although some works exist about $^{123/125/131}\text{I}$ radiolabeled DES [17], $^{131/125}\text{I}$ radiolabeled DES glucuronide derivatives [18] and also DES labeled with Auger emitters [19] we could not find any report about the radiolabeled phosphate derivatives of DES except Schomacker's study [20].

In the present study ^{99m}Tc was used, which is a radionuclide with a half-life of 6.02 h and plays an important

role in widespread applications of nuclear medicine [21, 22], but to date the authors are not aware of an existing study regarding ^{99m}Tc labeled phosphate derivative of DES, that is either provided with conjugation of phosphate group.

The aim of the present study was to synthesize phosphate derivative compound of DES [diethylstilbestrol diphosphate (DES-P)] and to label with ^{99m}Tc using tin chloride as reducing agent and to evaluate its in vivo biological activity in healthy male and female Wistar Albino rats.

Materials and methods

$\text{Na}^{99m}\text{TcO}_4$ was supplied by the Department of Nuclear Medicine of Ege University. DES was purchased from Sigma. All other chemicals were supplied from Merck Chemical Co and Aldrich Chemical Co. All animal experiments were carried out under the approval of to the relevant Institutional Animal Review Committee of Ege University, Turkey.

Equipments

Thin layer radio chromatograms (TLRC) and High-performance liquid chromatography (HPLC) chromatograms were obtained using a Cd(Te) detector equipped with a RAD 501 single-channel analyzer and HPLC instrument (LC-10ATvp quaternary pump and an auto sampler (SIL-20A HT) and 7.0 μm reversed-phase (RP)-C-18 column 250 \times 21 mm I.D., Macherey–Nagel) in Ege University Institute of Nuclear Sciences. Liquid chromatography mass spectrometry (LC/MS/MS) chromatograms were taken using an API 4000 LCMSMS Triple Quadrapole. Radio-TLC (Bioscan 2000) was in Ege University Institute of Nuclear Sciences.

Synthesis of DES-P

DES-P was synthesized according to the previous procedure with the Synkavit [23]. 1.39 g (0.10 mol) DES was dissolved in 4 mL pyridine and 5 mL POCl_3 was added to this solution drop by drop and stirred during one night at room temperature. After the reaction completed the pyridine was evaporated then 10 mL of dichloromethane and 10 mL of water was added. Thus the product was extracted to organic phase. The resulting supernatant (the organic phase) was separated and pH was adjusted to 9 by 3 M LiOH solution and the product was eluted using Dowex 50 column anion exchange column. The eluate was evaporated in water bath. Then the crude product was washed by 8 mL

ethanol and pH was adjusted to 10 by using 1 M NaOH. The mixture was purified by boiling with active carbon for 20 min and then the pure product was precipitated by evaporating ethanol.

Structural analysis

Liquid chromatography-mass spectrometry (LC/MS/MS)

The structure of DES-P was given in Fig. 1. LC/MS/MS spectra were taken using a Zivac TandemGold Triple Quadrupole LC/MS/MS. (m/z) values for DES, DES-P and some other fragments were presented in Fig. 2 and Table 1.

Nuclear magnetic resonance (NMR)

^1H -NMR (in D_2O) and ^{13}C -NMR (in Pyridine- D_5) spectra were taken in order to identify the chemical structure of DES-P. Both of the NMR spectra were obtained by using the facility of Erzurum Ataturk University, Faculty of Science and Department of Chemistry. Theoretical (ACD/LogP Algorithm Computer Programme) spectra were used for comparison with experimental NMR spectra (Tables 2, 3).

Spectrofotometric analysis of DES-P

Spectrofotometric analysis was performed to show the act of the alkaline phosphatase (ALP) enzyme on DES-P. ALP was dissolved with bidistilled water and aliquoted (100 μL), aliquots were stored at -80°C until use. Different concentrations ($1-10^{-9}$ μM) of DES solution were prepared, measured at 210 nm and calibration curve was drawn. Hundred microliters of ALP was activated with incubation at 37°C for 5 min. After activation substrate (1 μM DES-P) with pH 10 buffer was added quickly and spectrofotometric measurements until 15 min incubation were done with multiplate reader (Thermo Varioscan). Results of 15 min measurements graphed in Fig. 3.

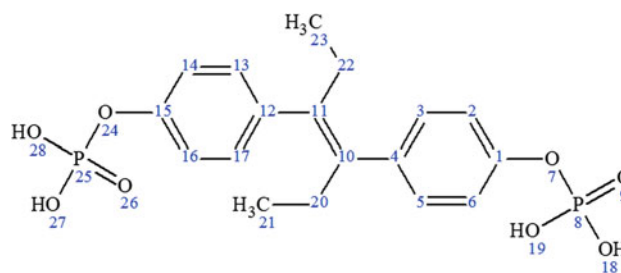


Fig. 1 Molecular structure of DES-P

Fig. 2 LC/MS/MS spectra (m/z) values for DES, DES-P and some other fragments

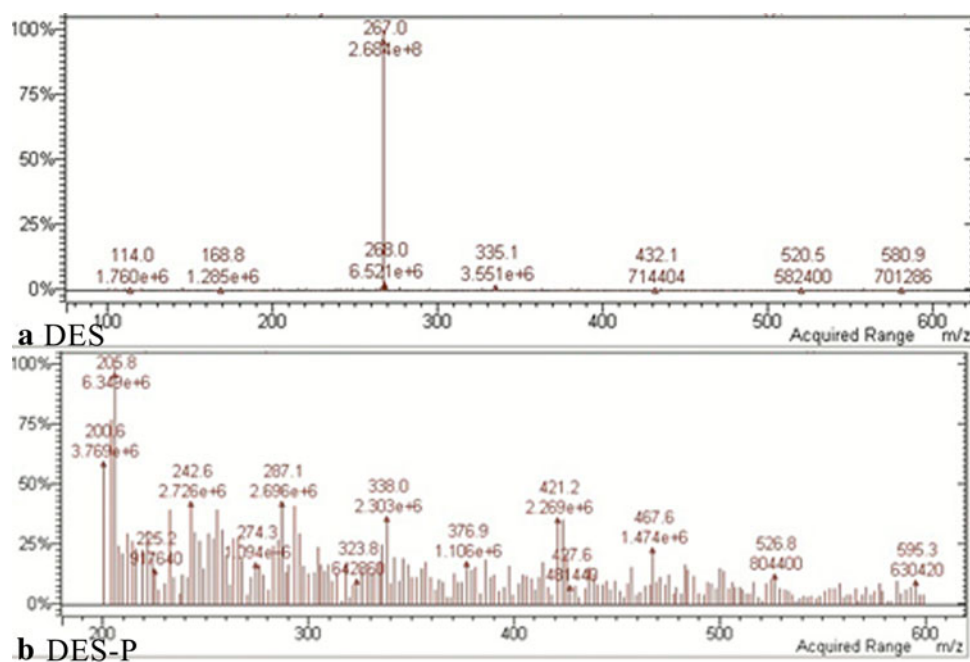


Table 1 LC/MS/MS spectra (m/z) values for DES, DES-P and some different fragments and proposed structures of selected fragments

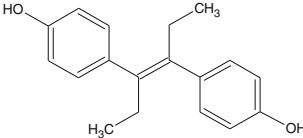
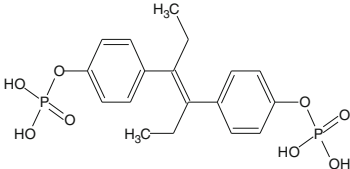
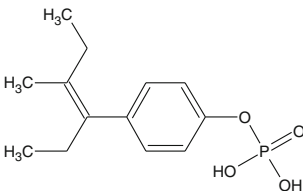
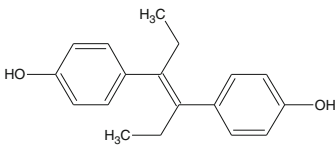
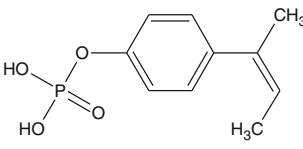
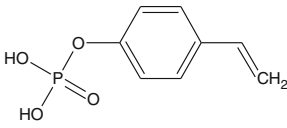
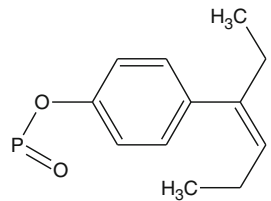
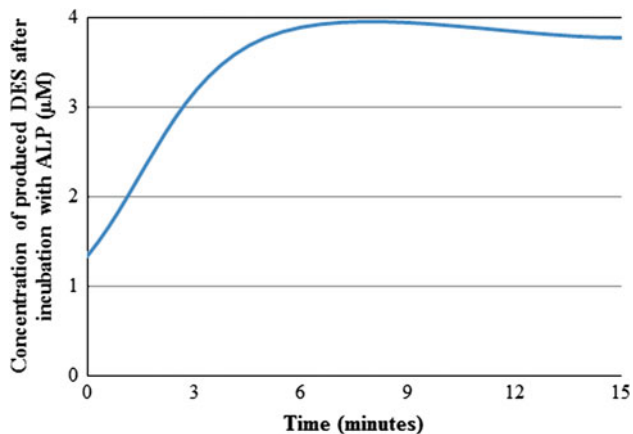
Fragment	m/z	Fragment	m/z
A	 268.35	E	 428.31
B	 270.26	F	 268.35
C	 228.18	G	 200.12
D	 222.22		

Table 2 Experimental and theoretical δ (ppm) values of ^{13}C -NMR (Pyridine- D_5) for DES-P

Carbon no.	Experimental	Theoretical
1, 15	149.63, 149.90	149.96, 149.98
10, 11	135.65	136.08
2, 6, 14, 16	123.57	119.63

Table 3 Experimental and theoretical δ (ppm) values of ^1H -NMR (D_2O) for DES-P

Carbon no.	Experimental	Theoretical
6, 14	7.00	6.96
5, 13	7.18, 7.17	7.26, 7.27
2, 16	6.99	6.99
17, 3	7.34, 7.37, 7.38	7.25, 7.26, 7.28
18, 19, 27, 28	4.70	4.51
20, 22	2.00, 2.02, 2.04, 2.09, 2.11, 2.16, 2.17, 2.21, 2.27	2.12, 2.13, 2.14, 2.15, 2.16, 2.18
21, 23	0.61, 0.62, 0.63, 0.65, 0.66	0.74, 0.75, 0.76, 0.77, 0.78, 0.79

**Fig. 3** Spectrophotometric analysis of ALP enzyme and DES-P

Radiolabeling of DES-P with $^{99\text{m}}\text{Tc}$

The stock solution of DES-P (500 $\mu\text{g}/0.50\text{ mL}$ bidistilled water) and SnCl_2 (1 mg/1 mL bidistilled water) were prepared. Then 0.10 mL DES-P and 100 μL SnCl_2 were mixed in a tube and pH was 7. One mCi (37 MBq)/100 μL of $^{99\text{m}}\text{TcO}_4^-$ were added into the mixture and incubated 20 min at room temperature. R_f value and % radiolabeling yield of $^{99\text{m}}\text{Tc}$ labeled DES-P ($^{99\text{m}}\text{Tc-DES-P}$) were

Table 4 R_f values of $^{99\text{m}}\text{TcO}_4^-$, Red. $^{99\text{m}}\text{Tc}$ and $^{99\text{m}}\text{Tc-DES-P}$

TLRC solvent	$^{99\text{m}}\text{TcO}_4^-$	Reduced $^{99\text{m}}\text{Tc}$	$^{99\text{m}}\text{Tc-DES-P}$
Mobile phase 1 ^a	0.93	1.00	0.07
Mobile phase 2 ^a	1.00	0.00	0.00

^a Mobile phase 1: Acid Citrate Dextrose (ACD); Mobile phase 2: Physiological serum (0.90% NaCl)

determined by Thin Layer Radio Chromatography (TLRC) method.

Quality control studies for $^{99\text{m}}\text{Tc-DES-P}$

Thin layer radio chromatography (TLRC) studies

TLRC was performed with ITLC-SG (Merck-5554) using $1.5 \times 10\text{ cm}$ size plates. Five μL aliquots of the samples ($^{99\text{m}}\text{TcO}_4^-$, Reduced $^{99\text{m}}\text{Tc}$ (Red. $^{99\text{m}}\text{Tc}$) and $^{99\text{m}}\text{Tc-DES-P}$) were applied to the plates 0.5 cm from the edge and placed in a tank containing the mobile phase, Acid Citrate Dextrose (ACD) and physiological serum (0.90% NaCl). Then, the TLRC plates were counted by TLC Scanner (BioscanAR 2000). R_f values of each component determined by the TLRC method. Table 4 shows R_f values of $^{99\text{m}}\text{TcO}_4^-$, Red. $^{99\text{m}}\text{Tc}$ and $^{99\text{m}}\text{Tc-DES-P}$.

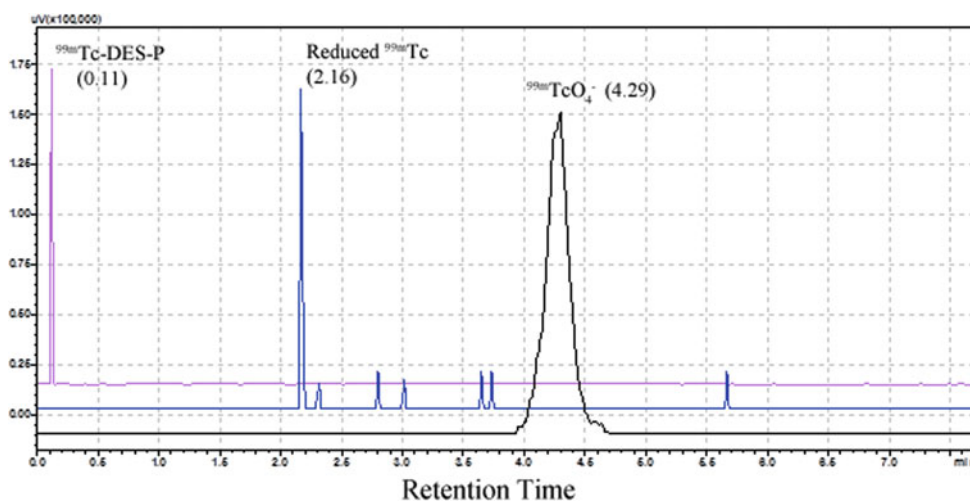
High performance liquid radio chromatography (HPLC) studies

A low pressure gradient HPLC system [LC-10ATvp quaternary pump and SPD-10A/V UV detector and an auto sampler (SIL-20A HT) and 5- μm RP-C18 column (250 \times 4.6 mm I.D., Macharey-Nagel)] was used for analytical experiments. The column was eluted with 65% methanol and bidistilled water with 0.1% TFA (v/v) at 0.8 mL/min. The eluted components were detected at 240 nm by UV detector SPD-10A/V. Figure 4 shows chromatograms of $^{99\text{m}}\text{TcO}_4^-$, Red. $^{99\text{m}}\text{Tc}$ and $^{99\text{m}}\text{Tc-DES-P}$.

Biodistribution studies on healthy Albino Wistar rats

Experiments with animals were approved by the Institutional Animal Review Committee of Ege University. $^{99\text{m}}\text{Tc}$ labeled DES-P was sterilized by passing through a 0.22 μm membrane filter. The activity was approximately 400 μCi (0.2 mL)/each rat. Then, it was injected into the tail vein of 9 male and 9 female healthy Wistar Albino rats (1 μg /each rat), which were 24 weeks old and with a weighed between 110 and 150 g. Receptor blocked ($^{99\text{m}}\text{Tc-Rec-DES-P}$)

Fig. 4 HPLC chromatogram of $^{99m}\text{TcO}_4^-$, Red. ^{99m}Tc and $^{99m}\text{Tc-DES-P}$



experiments were done by 10 μg of DES for each rats 15 min before the injection of $^{99m}\text{Tc-DES-P}$.

The rats were sacrificed at 30, 90 and 240 min post injection sodium pentobarbital (200 mg/kg) by intraperitoneal via, and tissues of interest were removed. Radioactivity was counted by a Cd(Te) detector equipped with a RAD 501 single channel analyzer. The percentage of injected dose per gram of tissue weight (%ID/g tissue) was determined.

Statistical analysis

Differences in the mean values of the measured activities were evaluated statistically by the SPSS 13 program (Univariate Variance Analyses and Pearson Correlation). Probability values <0.05 were considered significant. Pearson correlation was carried out among different organs for $^{99m}\text{Tc-DES-P}$.

Imaging studies on healthy female and male Albino Wistar rats

The imaging studies were performed on healthy female and male Albino Wistar rats ($n = 4$) in two groups (receptor blocked and unblocked). The static scintigrams were obtained using a gamma camera (Diacan Instruments) in Celal Bayar University, School of Medicine, Department of Nuclear Medicine. $^{99m}\text{Tc-DES-P}$ was sterilized by passing through a 0.22 μm membrane filter and injected into the tail vein of female and male Albino Wistar rats. A supplemental dose of alfazine and alfamine was used. The injected mass of $^{99m}\text{Tc-DES-P}$ was 5 μg /rats and the activity was approximately 3.7 MBq (100 μCi). For receptor blocked group 15 min before the injection of $^{99m}\text{Tc-DES-P}$, 50 μg of DES was injected to the rats. The scintigrams were obtained from anterior projection after different time intervals up to 2 h following the administration of $^{99m}\text{Tc-DES-P}$.

Results

Results of structural analysis

LC/MS/MS results

LC/MS/MS spectra confirmed expected molecular structure. According to LS/MS/MS results, the molecular fragments at m/z 267.00, 427.60 belong to DES and DES-P which could be shown by the structures in Fig. 2 and Table 1, respectively.

NMR results

Tables 2 and 3 represent experimental and theoretical δ (ppm) values of $^{13}\text{C-NMR}$ (Pyridine- D_5) and $^1\text{H-NMR}$ (D_2O), respectively, for DES-P. Experimental data were in agreement with the theoretical data, as expected. Both ^{13}C and ^1H NMR data showed that carbon no 18, 19, 27 and 28 confirmed phosphate group of DES-P.

Spectrofotometric analysis results of DES-P

The equation obtained from the calibration curve of the DES was $y = 0.52x + 0.29$ ($R^2 = 0.87$). The absorbance values of the ALP enzyme incubated with DES-P were 0.99, 2.25 and 2.25 for 0., 5.–15 min, respectively. It's seen that enzyme is cleaved the DES-P in 5 min.

Results of radiolabeling and quality control studies

TLRC

Radiolabeling yield of $^{99m}\text{Tc-DES-P}$ was found to be $99.00\% \pm 0.17$ ($n = 13$). As seen Table 4, R_f values of

Fig. 5 The ratio of the injected dose per gram (% ID/g) value of ER-rich tissues in male rats to % ID/g of muscle (Bg, background) for $^{99m}\text{Tc-DES-P}$ and $^{99m}\text{Tc-Rec-DES-P}$

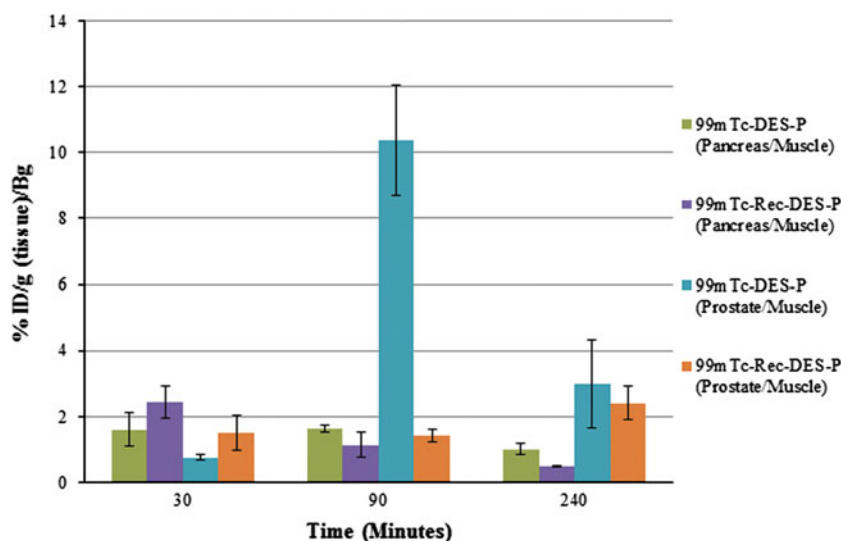


Fig. 6 The ratio of the injected dose per gram (% ID/g) value of ER-rich tissues in female rats to % ID/g of muscle (Bg, background) for $^{99m}\text{Tc-DES-P}$ and $^{99m}\text{Tc-Rec-DES-P}$

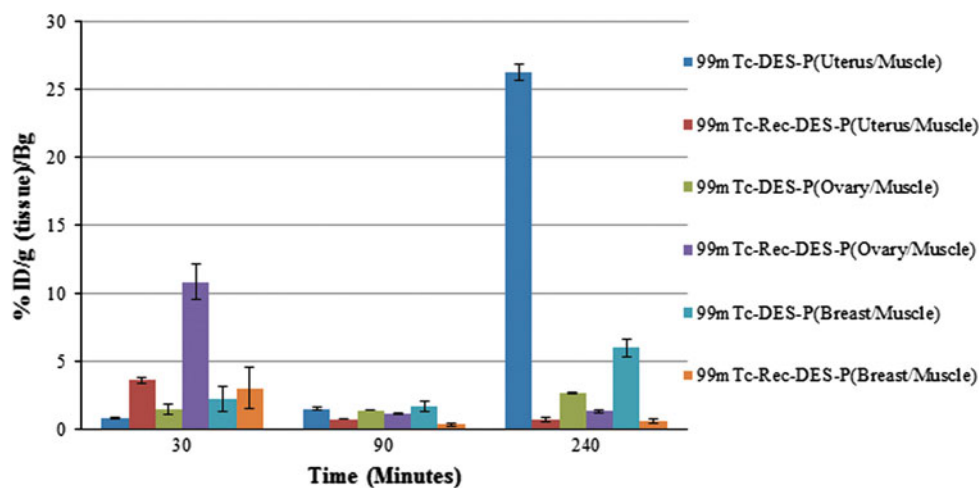


Table 5 The biodistribution (in % dose/g) of receptor blocked and unblocked studies with $^{99m}\text{Tc-DES-G}$ for various selected tissues in male rats ($n = 3$)

% ID/g	30 min		90 min				240 min					
	ER unblocked	SD	ER blocked	SD	ER unblocked	SD	ER blocked	SD	ER unblocked	SD	ER blocked	SD
Heart	3.41	2.36	5.27	2.58	1.06	0.06	0.27	0.10	7.91	0.42	0.50	0.20
Liver	3.77	1.96	14.13	3.84	7.07	3.26	32.91	1.37	3.85	0.17	7.12	0.15
Kidneys	18.86	2.68	10.26	0.01	6.35	1.13	1.40	0.33	11.15	4.56	3.43	1.38
S. Intestine	1.23	0.76	8.92	5.19	1.34	0.35	0.32	0.07	17.87	0.54	0.69	0.10
L. Intestine	2.41	1.32	7.42	0.60	3.34	0.36	0.22	0.02	13.61	3.16	0.72	0.40
Stomach	8.05	1.28	2.62	0.52	0.86	0.02	0.04	0.02	11.92	1.94	0.04	0.02
U. Bladder	81.60	41.74	46.25	13.93	1.63	0.36	5.44	2.15	81.10	17.05	1.17	0.05
Brain	0.47	0.20	0.23	0.10	0.05	0.02	0.02	0.00	0.29	0.01	0.02	0.01
Spleen	3.36	0.08	14.38	1.22	1.12	0.01	2.53	0.38	3.40	0.88	5.35	1.95

Table 6 The biodistribution (in % dose/g) of receptor blocked and unblocked studies with ^{99m}Tc-DES-G for various selected tissues in female rats (n = 3)

% ID/g	30 min				90 min				240 min			
	ER unblocked		SD ER blocked		ER unblocked		SD ER blocked		ER unblocked		SD ER blocked	
Heart	0.02	0.01	0.05	0.02	0.02	0.01	0.01	0.00	0.05	0.02	0.02	0.01
Liver	0.03	0.01	0.02	0.01	0.03	0.02	0.43	0.20	0.07	0.01	0.02	0.01
Kidneys	0.04	0.01	0.04	0.01	0.03	0.01	0.05	0.02	0.21	0.01	0.05	0.02
S. Intestine	0.06	0.02	0.12	0.07	0.03	0.02	0.06	0.02	0.07	0.03	0.04	0.02
L. Intestine	0.03	0.01	0.02	0.01	0.02	0.01	0.07	0.03	0.02	0.01	0.01	0.00
Stomach	0.03	0.00	0.16	0.07	0.04	0.02	0.07	0.02	0.03	0.01	0.01	0.00
U. Bladder	0.46	0.20	0.05	0.03	0.20	0.11	0.25	0.10	0.57	0.22	0.06	0.02
Brain	0.01	0.00	0.01	0.00	0.01	0.00	0.56	0.20	0.01	0.00	0.03	0.01
Spleen	0.03	0.00	0.04	0.01	0.01	0.00	0.02	0.00	0.05	0.02	0.02	0.01

^{99m}TcO₄⁻, Red. ^{99m}Tc and ^{99m}Tc-DES-P were 0.93, 1.00 and 0.07, respectively for mobile phase 1.

HPLRC

HPLRC chromatograms confirmed that a phosphate derivative of DES [Diethylstilbestrol diphosphate (DES-P)] was labeled with ^{99m}Tc successfully. The retention time (Rt) values of ^{99m}TcO₄⁻, Red. ^{99m}Tc and ^{99m}Tc-DES-P were different from each other (4.29, 2.16 and 0.11) as seen in Fig. 4.

Results of biodistribution studies

Biodistribution of ^{99m}Tc-DES-P as % injected dose/g tissue (%ID/g tissue) for male and female rats is given in Figs. 5 and 6 and Tables 5 and 6. When receptor blocked, male rats have higher uptake values than females in period time.

^{99m}Tc-DES-P was eliminated through the kidneys and accumulated in bladder in both male and female rats for receptor unblocked and blocked studies. Small intestines uptakes in male rats were significantly higher (p < 0.05) than females. Uterus uptake was ~26 times less when receptor blocked within 240 min post injection. Similarly small and large intestines uptakes were decreased 26 and 19 times when ER receptors blocked.

No significant radioactivity uptakes were seen in brain of both sexes.

Figure 5 demonstrates the ratios of the injected doses per gram (% ID/g) to % ID/g of muscle (Bg, background) for ER-rich tissues in male rats. Prostate uptake was ~3.50 times less than from 90 min to 240 min postinjection (p < 0.05).

The ratio of the injected dose per gram (% ID/g) for ER-rich tissues in female rats to % ID/g of muscle for ^{99m}Tc-DES-P and ^{99m}Tc-Rec-DES-P can be seen in Fig. 6.

The uterus/muscle ratios when estrogen receptors unblocked are 0.89, 1.55, 26.25 in 30, 90 and 240 min, respectively. These results indicate that the ^{99m}Tc-DES-P has been uptaken significantly by the uterus tissue within 240 min.

Bone to muscle ratios for ^{99m}Tc-DES-P/^{99m}Tc-Rec-DES-P are given in Fig. 7. The bone/muscle ratios of female rats were significantly higher than the male rats’ the bone/muscle ratios at 90 min and 240 min. Female rats’ the bone/muscle ratio presented 15.14 times higher than male rats’ the bone/muscle ratio at 90 min postinjection particularly.

Results of imaging studies

Ratio of the bony regions’ ROI values of ^{99m}Tc-DES-P/^{99m}Tc-Rec-DES-P for female and male rats is given in

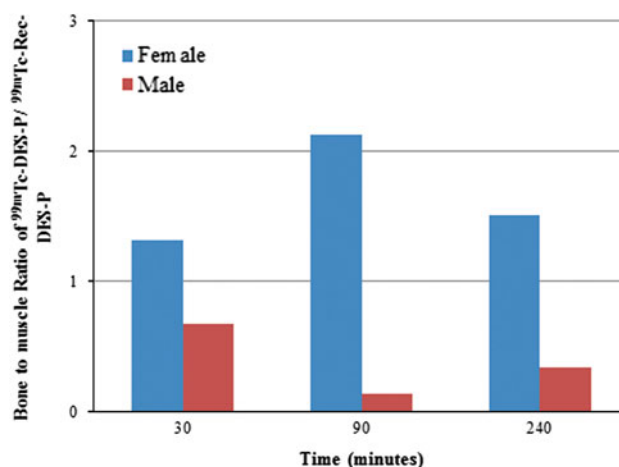


Fig. 7 Bone to muscle (Bg, background) % ID/g ratio of ^{99m}Tc-DES-G and ^{99m}Tc-Rec-DES-G for female and male rats

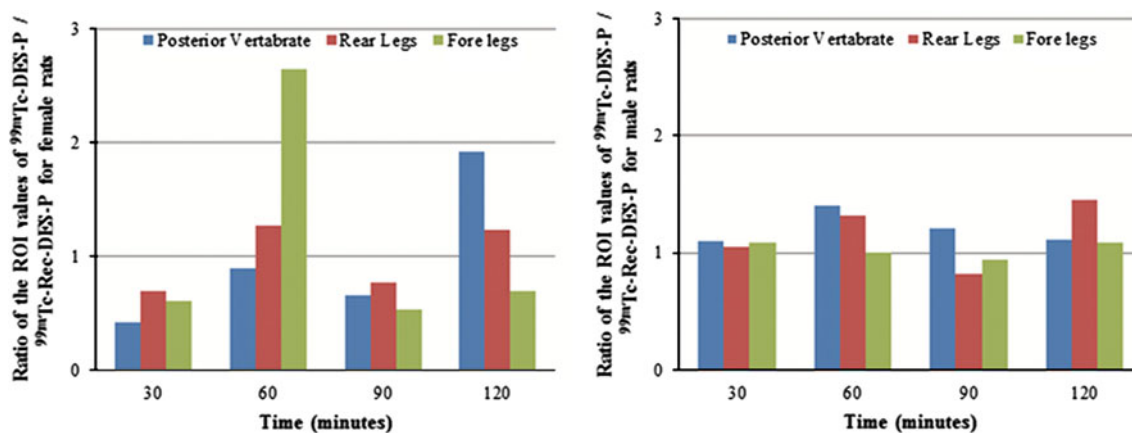


Fig. 8 Ratio of the ROI values of $^{99m}\text{Tc-DES-P}/^{99m}\text{Tc-Rec-DES-P}$ for female and male rats

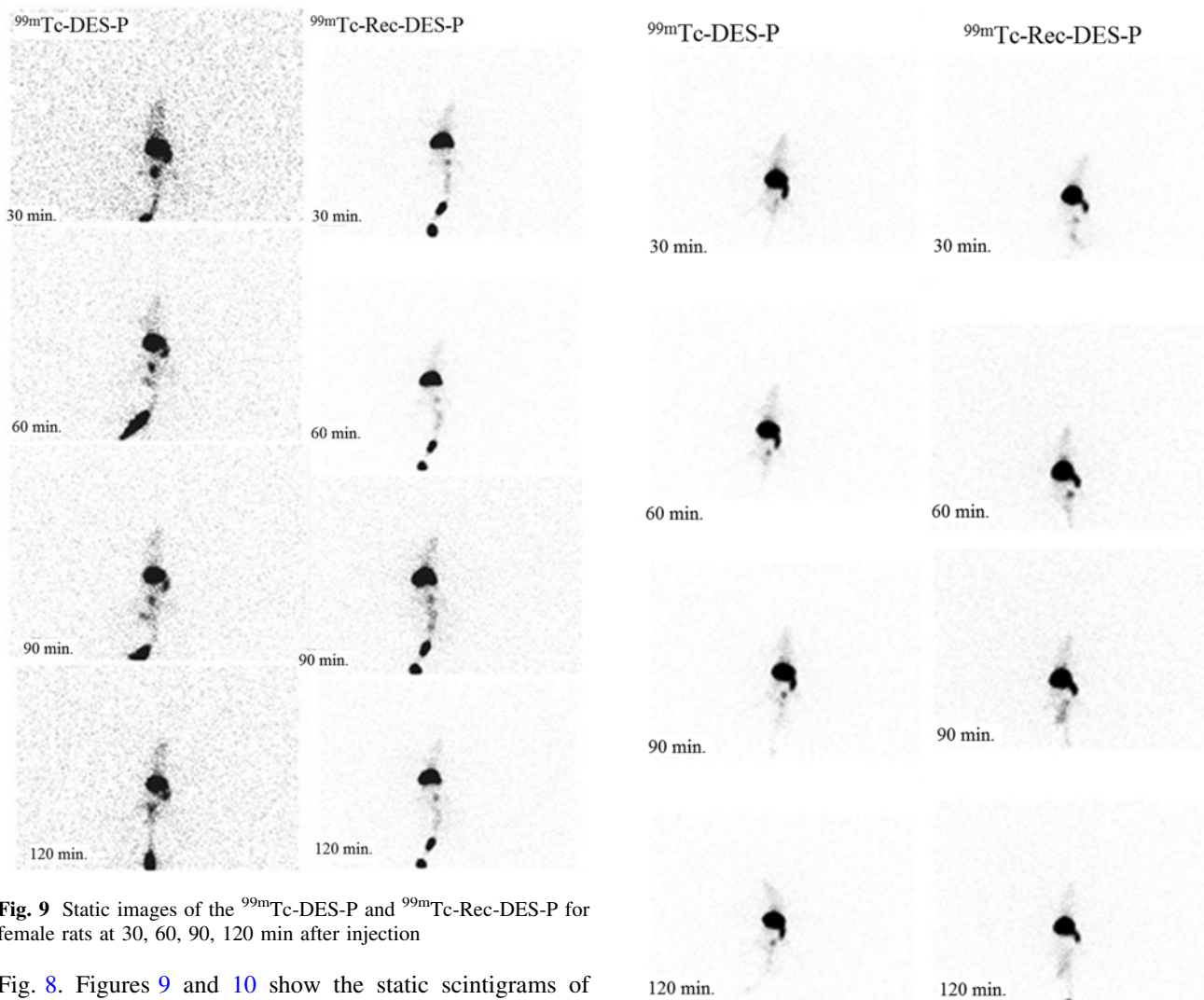


Fig. 9 Static images of the $^{99m}\text{Tc-DES-P}$ and $^{99m}\text{Tc-Rec-DES-P}$ for female rats at 30, 60, 90, 120 min after injection

Fig. 8. Figures 9 and 10 show the static scintigrams of female and male rats corresponding to 30, 60, 90 and 120 min after the administration of $^{99m}\text{Tc-DES-P}$. When Figs. 7 and 8 were taken into consideration, uptake of bony

Fig. 10 Static images of the $^{99m}\text{Tc-DES-P}$ and $^{99m}\text{Tc-Rec-DES-P}$ for male rats at 30, 60, 90, 120 min s after injection

regions was similar within 60 and 120 min. Particularly, the uptake of bony regions for female rats was higher than male rats' uptake in these time period. As seen in Figs. 9 and 10 there were high accumulation in the kidneys, liver and spleen. This accumulation lowered within 120 min. Furthermore, posterior vertebrate accumulation was noteworthy. The primary excretion route for both female and male rats was kidneys.

Discussion

Fischer calculated the highest radiolabeling yields for $^{123/125/131}\text{I}$ radiolabeled DES [17]. Yilmaz' results were 93% and 81% for ^{131}I labeled DES and ^{131}I labeled DES-glucuronide, respectively [18]. In our study, radiolabeling yield of $^{99\text{m}}\text{Tc}$ -DES-P was found to be $99.00\% \pm 0.17$ ($n = 13$).

$^{99\text{m}}\text{Tc}$ -DES-P was eliminated through the kidneys and accumulated in the bladder in both male and female rats. The uptakes for the both sexes could be due to the conjugation of phosphate group. Hepatobiliary excretion was also observed. In literature, it is known that fosfestrol is metabolized to DES by phosphatase mainly in the liver and DES is eliminated into urine or feces [24].

Glucuronide conjugates of steroids were excreted in the bile and hence, in the intestines [25]. Some glucuronide derivatives DES-P [18], TAM-G [26], and other aglycon glucuronides [27–34] were reported in the literature. They have high intestinal system and urinary bladder uptakes.

In our study prostate uptake of $^{99\text{m}}\text{Tc}$ -DES-P was elevated in 90 min. Schomacker et al. reported that ^{123}I radiolabeled diethylstilbestrolphosphate (DESP) was accumulated in ER rich tissues of prostate from 10 min up to 2 h post injection [20].

$^{99\text{m}}\text{Tc}$ -DES-P has also a significant uptake by the uterus tissue within 240 min. Yilmaz reported that ^{131}I radiolabeled DESG have receptor affinity on uterus, ovaries and breast tissues according to biodistribution studies with female Wistar Albino rats [18].

Conclusion

The results showed that DES-P could be successfully radiolabeled with $^{99\text{m}}\text{Tc}$. The biodistribution studies showed that DES-P is ER specific. The bones uptake increased within 90 min. postinjection. It may potentially be proposed as a $^{99\text{m}}\text{Tc}$ labeled imaging agent for alkaline phosphatase enzyme rich tumors and also estrogen receptor rich tissues such as uterus, prostate and bones.

Further studies with animal models with tumors and cell culture experiments should be done in order to explore if

$^{99\text{m}}\text{Tc}$ -DES-P may be used as an imaging agent, early tumor detection and metastasis tumors.

Acknowledgments The authors thank the financial support from Ege University Scientific Research Fund with the Project Number 2009NBE001. Authors thank to Dr. Memduh Bülbül for providing ALP.

References

- Weihua Z, Andersson S, Cheng G, Simpson ER, Warner M, Gustafsson JA (2003) Update on estrogen signaling. *FEBS Lett* 546:17–24
- Kohler BA, Ward E, McCarthy BJ, Schymura MJ, Ries LA, Ehemann C, Jemal A, Anderson RN, Ajani UA, Edwards BK (2011) Annual report to the nation on the status of cancer, 1975–2007, featuring tumors of the brain and other nervous system. *J Natl Cancer Inst* 103:714–736
- Yan-Qing Q, Zhong-Ze F, Yang LV, Zhen-Ming G, Rui L, Liang-Liang Z, Pei-Pei D, Yan-Yan Z, Guang-Bo G, Li-Ming W (2011) Reversible inhibition of four important human liver cytochrome P450 enzymes by diethylstilbestrol. *Pharmazie* 66:216–221
- Yu S, Zhang Y, Yuen MT, Zou C, Danielpour D, Chan FL (2011) 17-Beta-estradiol induces neoplastic transformation in prostatic epithelial cells. *Cancer Lett* 304:8–20
- Saeed M, Rogan E, Cavalieri E (2009) Mechanism of metabolic activation and DNA adduct formation by the human carcinogen diethylstilbestrol: the defining link to natural estrogens. *Int J Cancer* 124:1276–1284
- Themelis DG, Trellopoulos AV, Tzanavaras PD, Karlberg B (2005) Assay of the synthetic estrogen fosfestrol in pharmaceutical formulations using capillary electrophoresis. *J Pharm Biomed Anal* 39:559–563
- Tzanavaras PD, Themelis DG, Karlberg B (2002) Rapid spectrophotometric determination of fosfestrol following on-line hydrolysis by alkaline phosphatase using flow injection and chasing zones. *Anal Chim Acta* 462:119–124
- Tzanavaras PD, Themelis DG (2003) Flow injection spectrophotometric determination of fosfestrol, following on-line thermal induced digestion and using an orthophosphate calibration graph. *Talanta* 59:207–213
- Droz JP, Kattan J, Bonnay M, Chraïbi Y, Bekradda M, Culine S (1993) High-dose continuous-infusion fosfestrol in hormone-resistant prostate cancer. *Cancer* 71:1123–1130
- Azuma H, Sakamoto T, Kiyama S, Ubai T, Kotake Y, Inamoto T, Takahara K, Nishimura Y, Segawa N, Katsuoka Y (2008) Anti-cancer effect of combination therapy of VP16 and fosfestrol in hormone-refractory prostate cancer. *Am J Clin Oncol* 31:188–194
- Williams AR, Whelan P (1998) Use of intravenous fosfestrol tetrasodium (Honvan) infusion in treatment of symptomatic advanced prostate cancer. *Prostate Cancer Prostatic Dis* 1:204–207
- Khalaf A, Pfister C, Hellot MF, Dunet F, Moussu J, Grise P (2002) Value of mitoxantrone in metastatic hormone-resistant prostate cancer. *Prog Urol* 12:37–42
- Simic T, Dragicevic D, Savic-Radojevic A, Cimbaljevic S, Tulic C, Mimic-Oka J (2007) Serum gamma glutamyl-transferase is a sensitive but unspecific marker of metastatic renal cell carcinoma. *Int J Urol* 14:289–293
- McKee M (2008) Extracellular matrix proteins, alkaline phosphatase and pyrophosphate as molecular determinants of bone, tooth, kidney and vascular calcification. *Renal Stone Disease 2 Book Series: AIP Conference Proceedings*, vol 1049, pp 25–32

15. Brun-Heath I, Ermonval M, Chabrol E, Xiao J, Palkovits M, Lyck R, Miller F, Couraud PO, Mornet E, Fonta C (2011) Differential expression of the bone and the liver tissue non-specific alkaline phosphatase isoforms in brain tissues. *Cell Tissue Res* 343:521–536
16. Beortsen W, Van den Bos T (1992) Alkaline phosphatase induces the mineralization of sheets of collagen implanted subcutaneously in the rat. *J Clin Invest* 89:1974–1980
17. Fischer T, Schomacker K, Schicha H (2004) Labelling purification and receptor affinity of radioactive iododiethylstilbestrol (*I-DES) with high specific activity and first structure analysis with natI-DES. *J Label Compd Radiopharm* 47:669–678
18. Yılmaz T (2010) Manyetik nanoparçacıklara bağlı $^{125}\text{I}/^{131}\text{I}$ işaretli dietilstilbestrol (DES) glukuronid'in sentezlenmesi, biyolojik etkinliğinin incelenmesi. EÜ Fen Bil Enstitüsü
19. Fischer T, Schomacker K, Schicha H (2008) Diethylstilbestrol (DES) labeled with Auger emitters: potential radiopharmaceutical for therapy of estrogen receptor-positive tumors and their metastases? *Int J Radiat Biol* 84:1112–1122
20. Schomacker K, Meller-Rehbein B, Gabruk-Szostak B, Gerard H, Scheidhauer K, Scharl A (1997) Investigations into biokinetics of I-123 Diethylstilbestrol phosphate in tumour-bearing mice. *Radioactive isotopes in clinical medicine and research*, pp 333–342
21. Rossin R, Rebonato J, Bello M, Coradini D, Pellizzaro C, Perbellini A, Mazzi U, Nicolini M (2002) Technetium, Rhenium and Other Metals in Chemistry and Nuclear Medicine (Padova: SGEEditoriali), pp 399–402
22. Méndez-Rojaz MA, Kharisov BI, Tsivadze AY (2006) Recent advances on technetium complexes: coordination chemistry and medical applications. *J Coord Chem* 59:1–63
23. Unak T, Unak P (1993) Synkavit and its direct labelling with iodine-125, as a potential anti-cancer drug. *Nucl Med Biol* 20:889–894
24. Motoaki H, Yoshihiro T, Hidetoshi Y (2001) The pharmacokinetics of fosfestrol and diethylstilbestrol in chronic hemodialysis patients with prostate cancer. *Int J Urol* 8:681–685
25. Unak T, Avcıbaşı U, Yıldırım Y, Cetinkaya B (2003) Attempts to develop a new nuclear measurement technique of β -glucuronidase levels in biological samples. *Czechoslovak J Phys* 53:A797–A802
26. Biber Muftuler FZ, Unak P, Ichedef Ç, Demir I (2011) Synthesis of a radioiodinated antiestrogen glucuronide compound. *J Radioanal Nucl Chem* 287:679–689
27. Unak T, Unak P, Ongun B, Duman Y (1997) Synthesis and iodine-125 labelling of glucuronide compounds for combined chemo- and radiotherapy of cancer. *Appl Radiat Isot* 48:777–783
28. Biber FZ, Unak P, Ertay T, Medine EI, Zihnioglu F, Tasci C, Durak H (2006) Synthesis of an estradiol glucuronide derivative and investigation of its radiopharmaceutical potential. *Appl Radiat Isot* 64:778–788
29. Ertay T, Ünak P, Tasci C, Biber FZ, Zihnioglu F, Medine EI, Durak H (2006) $^{99\text{m}}\text{Tc}$ -Exorphin-glucuronide in tumor diagnosis: preparation and biodistribution studies in rats. *J Radioanal Nucl Chem* 269:21–28
30. Enginar H, Ünak P, Biber Müftüler FZ, Lambrecht FY, Medine EI, Yolcular S, Yurt Kilcar A, Seyitoğlu B, Bulduk İ. (2011) Synthesis, radiolabelling and biodistribution of morphine glucuronide (mor-glu). *J Radioanal Nucl Chem*. doi:10.1007/s10967-011-1412-4
31. Koçan F, Avcıbaşı U, Ünak P, Müftüler FZB, Ichedef ÇA, Demiroğlu H, Gümüşer FG (2011) Metabolic comparison of radiolabeled bleomycin (BLM) and bleomycin-glucuronide (BLMG) labeled with $^{99\text{m}}\text{Tc}$. *Cancer Biother Radiopharm* 26: 573–584
32. Medine IE, Unak P, Sakarya S, Toksoz F (2010) Enzymatic synthesis of uracil glucuronide, labeling with $^{125}/^{131}\text{I}$, and in vitro evaluation on adenocarcinoma cells. *Cancer Biother Radiopharm* 25:335–344
33. Teksoz S, Ichedef CA, Ozyuncu S, Muftuler ZB, Unak P, Medine EI, Ertay T, Eren MS (2011) $^{99\text{m}}\text{Tc}$ -D-Penicillamine-Glucuronide: synthesis, radiolabeling, in vitro and in vivo evaluation. *Cancer Biother Radiopharm* 26:1–8
34. Yesilgac R, Unak P, Medine EI, Ichedef CA, Ertay T, Muftuler FZ (2011) Enzymatic synthesis of $(^{125}/^{131}\text{I})$ labeled 8-hydroxyquinoline glucuronide and in vitro/in vivo evaluation of biological influence. *Appl Radiat Isot* 69:299–307